doi:10.1016/j.jmb.2008.09.003 J. Mol. Biol. (2009) 387, 965–974

JMB

Available online at www.sciencedirect.com

ScienceDirect

ELSEVIER

Mutational Analysis of the Aggregation-Prone and Disaggregation-Prone Regions of Acylphosphatase

Martino Calamai[1], Gian Gaetano Tartaglia[1], Michele Vendruscolo[1], Fabrizio Chiti[2,3] and Christopher M. Dobson[1]*

[1]*Department of Chemistry, University of Cambridge, Lensfield Road, Cambridge CB2 1EW, UK*

[2]*Dipartimento di Scienze Biochimiche, Università degli Studi di Firenze, Viale Morgagni 50, 50134 Florence, Italy*

[3]*Consorzio interuniversitario "Istituto Nazionale Biostrutture e Biosistemi" (I.N.B.B.), Viale delle Medaglie d'Oro, 305, 00136 Rome, Italy*

Received 17 March 2008; received in revised form 8 July 2008; accepted 3 September 2008
Available online 12 September 2008

Edited by S. Radford

We have performed an extensive mutational analysis of aggregation and disaggregation of amyloid-like protofibrils of human muscle acylphosphatase. Our findings indicate that the regions that promote aggregation in 25% (v/v) 2,2,2 trifluoroethanol (TFE) are different from those that promote disaggregation under milder conditions (5% TFE). Significant changes in the rate of disaggregation of protofibrils in 5% TFE result not only from mutations situated in the regions of the sequence that play a key role in the mechanism of aggregation in 25% TFE, but also from mutations located in other regions. In order to rationalise these results, we have used a modified version of the Zyggregator aggregation propensity prediction algorithm to take into account structural rearrangements of the protofibrils that may be induced by changes in solution conditions. Our results suggest that a wider range of residues contributes to the stability of the aggregates in addition to those that play an important kinetic role in the aggregation process. The mutational approach described here is capable of providing residue-specific information on the structure and dynamics of amyloid protofibrils under conditions close to physiological and should be widely applicable to other systems.

Keywords: amyloid; protein misfolding; aggregates disassembly; TFE; computational prediction

Introduction

Research on protein misfolding and aggregation is becoming progressively more intense, largely because of its impact on our understanding at a molecular level of the causes of widespread and highly debilitating neurodegenerative human pathologies such as Alzheimer's and Parkinson's diseases.[1–3] Protein aggregates associated with such diseases, known as amyloid fibrils when they deposit in the extracellular space or inclusion bodies when they accumulate intracellularly, are often fibrillar in morphology and have a cross-β structure in which β-strands are oriented perpendicular to the fibril axis.[4–6] It has been found, however, that formation of these fibrils is not a feature limited to a few proteins or peptides associated with disease, but is a common characteristic of polypeptide chains, as an increasing number of peptides and proteins unrelated to any pathological condition have been found to form similar structures *in vitro* when appropriate conditions are chosen.[6,7] The study of the mechanisms of amyloid formation therefore provides fundamental information about the nature and evolution of functional states of proteins.[8]

Mutational studies have proved to be extremely valuable for the characterisation of amyloid fibrils and the process of their formation. Structural information concerning fibrils formed from the Aβ peptide, α-synuclein and tau has been determined with the use of scanning cysteine or proline mutagenesis and labelling the cysteine residues with spin probes or other agents.[9–13] More recently, scanning alanine mutagenesis has been employed to validate the structural model of the amyloid protofilament formed by the second WW domain of CA150 obtained through solid-state NMR spectroscopy.[14] Such success indicates that mutational

**Corresponding author.* E-mail address: cmd44@cam.ac.uk.

Abbreviations used: TFE, 2,2,2 trifluoroethanol; AcP, acylphosphatase; ThT, thioflavin T; wt, wild type.

studies have the potential to provide residue-specific structural information on the process of amyloid formation, even for relatively large proteins. In order to explore the possibility of using such information to provide further insight into the mechanism of fibril formation and the origin of fibril stability, in the present study we have extended this type of approach by investigating the effect of single amino acid substitutions on the rates of disaggregation of amyloid structures of human muscle acylphosphatase (AcP), a protein not associated with any known disease, but which has been shown to form amyloid-like fibrils *in vitro* under destabilising conditions, e.g., in the presence of 25% (v/v) 2,2,2 trifluoroethanol (TFE).[15]

The aggregation of this protein has already been studied in detail by a wide variety of methods including extensive mutational analysis.[16–21] In addition to such studies, we have recently demonstrated that the aggregation process is reversible to an extent that depends on the time that aggregation has been allowed to occur and on the size of the aggregates that are formed.[22] In particular, AcP forms well-defined protofibrillar species in 25% (v/v) TFE solution prior to the formation of mature fibrils. We have shown that when such species are transferred to a solution containing just 5% (v/v) TFE, a concentration at which the native structure of AcP is more stable than the unfolded state,[23] the aggregates disassemble and the resulting monomeric protein can subsequently refold to the native state.[22] One of the advantages of studying disaggregation is that this process may occur under conditions close to physiological, as opposed to those that favour protofibril formation that involve harsher conditions such as the presence of chemical denaturants.

In the present study, we have used a battery of 50 mutants that result in changes in hydrophobicity, secondary-structure propensity and net charge. Our data show that dramatic changes in the rate of disaggregation of preformed protofibrils result from mutations situated in the aggregation-promoting regions in 25% TFE[17] as well as additional regions that do not play an important kinetic role in the aggregation process. These results suggest the contribution of a wider range of residues to the stability of the protofibrils.

Results and Discussion

Mutational studies of protein aggregation and disaggregation

It is increasingly clear that the small aggregates formed prior to well-defined amyloid fibrils are the primary species giving rise to cellular toxicity.[3] The conditions used in this study were therefore chosen to probe the character of amyloid-like protofibrils rather than mature fibrils. In 25% (v/v) TFE, AcP converts from an ensemble of partially unfolded conformations into protofibrillar aggregates that contain a significant amount of β-sheet structure and bind to thioflavin T (ThT); this process shows apparent single-exponential kinetics when monitored with ThT fluorescence.[17] All the substantial conformational rearrangements at a molecular level are achieved after incubating wild-type (wt) AcP in 25% (v/v) TFE for 70 min at a concentration of 0.4 mg/ml in 25% (v/v) TFE, 50 mM sodium acetate, pH 5.5, 25 °C.[22] When the wt protein was incubated for longer than 70 min, only changes in the degree of assembly of the aggregates were observed.

In this work, the mutants were incubated in 25% TFE for times proportional to 70 min (t^1_{agg} of Fig. 1) to obtain protofibrillar species structurally similar to those formed by wt AcP. The appropriate time of aggregation of each mutant was calculated from its aggregation rate constant and the relative ThT fluorescence intensity of wt AcP after 70 min

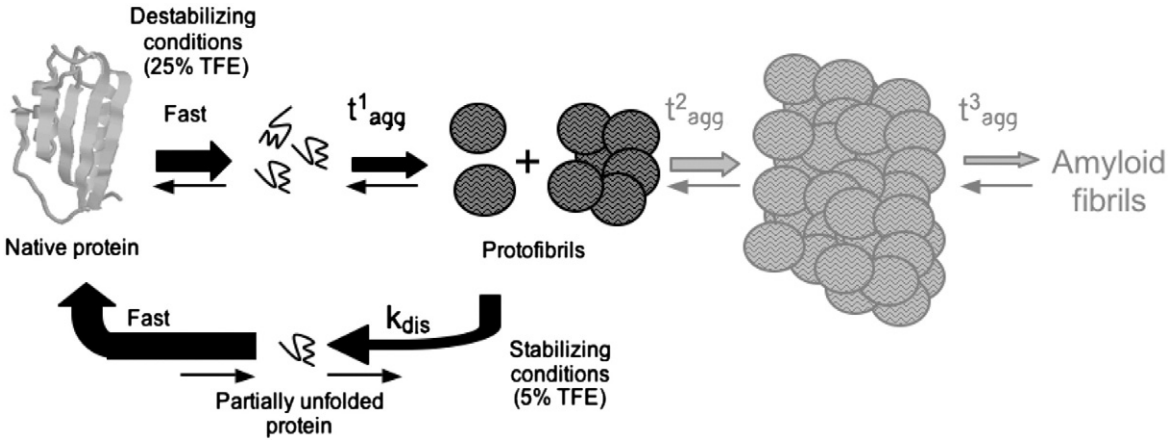

Fig. 1. Schematic illustration of the aggregation and disaggregation processes of AcP. Addition of 25% (v/v) TFE induces the partial unfolding of native AcP and the subsequent conversion (with characteristic times t^1_{agg} and t^2_{agg}) into early amyloid aggregates. At a later stage (t^3_{agg}), mature amyloid fibrils develop. After incubation times long enough to obtain a protein population rich in protofibrils (t^1_{agg} = 70 min for wild-type AcP), the samples are transferred to a solution containing 5% (v/v) TFE. Under these conditions, the aggregates of wild-type AcP and its variants disassemble with well-defined rate constants (k_{dis}) and the resulting monomeric protein can subsequently refold to the native state.

incubation in 25% TFE (see Materials and Methods for details). A possible approach to comparing the residues involved in the kinetics of formation and disassembly of the protofibrils would have been to promote aggregation of the various mutants in 25% TFE and then induce disaggregation by reducing then protein concentration while keeping the concentration of TFE at 25%. Nevertheless, we could not observe any significant disaggregation taking place in 25% TFE, even after a 50-fold dilution of the pre-aggregated protein sample. We could not decrease the protein concentration further because of the limit of resolution when intrinsic fluorescence or ThT was used as a probe to monitor disaggregation. A relatively fast disassembly of AcP protofibrils followed by refolding to the native state can, however, be observed when the concentration of TFE is reduced to 5%.[22]

Each solution containing the protofibrils of wt or mutant AcP was therefore diluted fivefold to give a final protein concentration of 0.08 mg/ml in 5% TFE and 50 mM sodium acetate, pH 5.5, at 25 °C. Disaggregation was studied by monitoring changes in the intensities of both ThT and intrinsic fluorescence, as described previously for the wild-type protein[22] (Fig. 2a and b). The kinetic traces were highly reproducible (Fig. S1), and the disaggregation rate constants determined from the two methods were similar, although the rate constants obtained from changes in intrinsic fluorescence intensity were systematically slightly higher (~10%). Under the disaggregation conditions used here, the samples contain predominantly small aggregated species with a similar structural organization and a single-exponential function can describe well the data. The mean of the rate constants obtained with the use of ThT and intrinsic fluorescence was taken as the value of the disaggregation rate constant for each mutant. As the fraction of aggregated material that disaggregated within the time scale of the experiment was found to vary, only those protein variants for which at least 20% disassembly was observed during the time scale used here were included in the kinetic analysis (Fig. 2c).

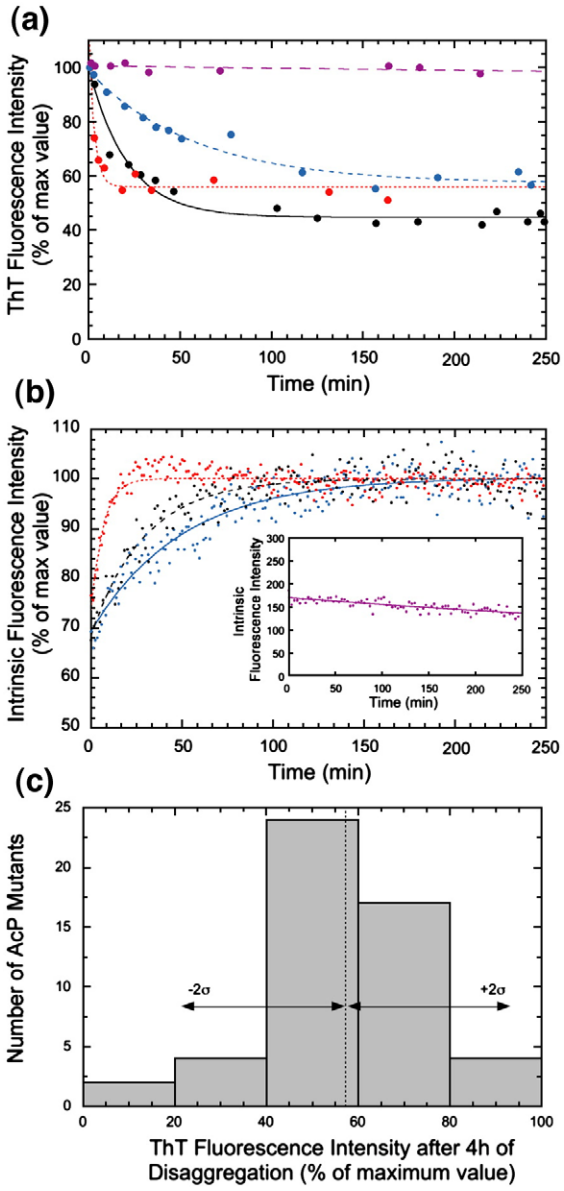

Fig. 2. Disaggregation kinetics followed by ThT (a) and intrinsic fluorescence intensity (b). Wild-type AcP and its variants were incubated at a concentration of 0.4 mg/ml in 25% (v/v) TFE. After incubation of each mutant for an equivalent time (see the text), samples were diluted fivefold to a final concentration of 0.08 mg/ml in 5% (v/v) TFE. Wild-type, black; K44E, blue; E29R, red; F94L, purple. The continuous lines represent the single-exponential functions that best fit the data. (c) Number of AcP variants against the decrease in ThT fluorescence intensity following 4 h of disaggregation. Only mutants with values falling within two standard deviations from the mean were considered to undergo the process of disaggregation from the same type of early aggregates and hence with the same mechanism ($n = 51$, mean = 57.2%, SD = 18.0%).

Regions governing the disaggregation of protofibrils

We investigated first the effects of 31 single point mutations involving changes in hydrophobicity and secondary-structure propensity but not charge. The mutations were located at various positions along the sequence of AcP and were the same as those used to determine the effect of amino acid substitutions on the rate of aggregation of AcP.[17] As shown in Fig. 3a, disaggregation rates significantly different from that of the wt protein were found for 12 out of 15 mutants bearing a single amino acid replacement in the region 7–49 (V9A, Y11F, V17A, V20A, F22L, Y25A, A30G, G34A, V36A, V39A, T42A, V47A) and for four mutants out of six in the region 84–98 (I86V, S87T, Y91Q, Y98Q). By contrast, six out of eight mutants involving the regions 1– 6 and 50–83 appeared to disaggregate, within experimental error, at a rate comparable to that of the wt protein [$\ln(v_{mut}/v_{wt})^{dis} \sim 0$]. The experimental measurements reported here show therefore that mutations within regions 7–49 and 84–98 generally change the disaggregation rate significantly, indicating that these regions are likely to be structured within the aggregates in 5% TFE. By

contrast, mutations within the regions 1–6 and 50–83 do not have significant effects on disaggregation and are therefore likely to be poorly structured in the protofibrillar aggregates.

Two mutants, E29D and F94L, did not show any decrease in ThT fluorescence intensity or increase in intrinsic fluorescence intensity during the experiments, indicating that no significant disaggregation took place on the time scale monitored here (Fig. 2a and b). We suggest that these mutations could shorten the time (t^2_{agg} of Fig. 1) required for the conversion from the initially formed amyloid fibril precursors into larger assemblies, as the latter aggregates have previously been shown to be highly resistant to disaggregation.[22] Alternatively, these mutations could also contribute to the stabilization of the early aggregates by promoting a particularly favourable packing of the residues. At present our data are, however, not conclusive enough to discriminate between these two hypotheses.

Identification of the major factors that influence the process of aggregation, such as hydrophobicity, secondary-structure propensity, net charge[24] and regions of alternating hydrophobic and hydrophilic residues,[25] has led to the development of algorithms able to predict the regions of the sequence of a given protein that are likely to have a high intrinsic aggregation propensity.[26–30] The calculation of the aggregation propensity profile of a protein in the presence of TFE should take into account the fact that the intrinsic propensities for secondary-structure formation and the hydrophobicity scale are very significantly altered by the presence of TFE. In this study, we have therefore developed a specific version of the previously published Zyggregator algorithm[26,31] in order to obtain the aggregation propensity profile of AcP in the presence of TFE (see Materials and Methods).

The aggregation propensity profile calculated for AcP using the new version of the algorithm, which considers for the computation the protein as unstructured and in 5% TFE, features five major peaks at positions 8–12, 21–25, 35–37, 45–50 and 88–98 (Fig. 3b). These peaks, which would correspond to regions of the sequence promoting aggregation and forming the β-sheet structure in the resulting aggregates,[26] are all located within the regions encompassing residues 7–49 and 84–98 that appear to be structured from the mutational analysis presented here (Fig. 3a and b). Moreover, no peaks are apparent at the N-terminus (residues 1–6) and in the large central region (residues 50–83), in agreement with the lack of mutational effects in these regions (Fig. 3a and b).

Taken together, these data show that the regions of the sequence that affect the disaggregation rate upon

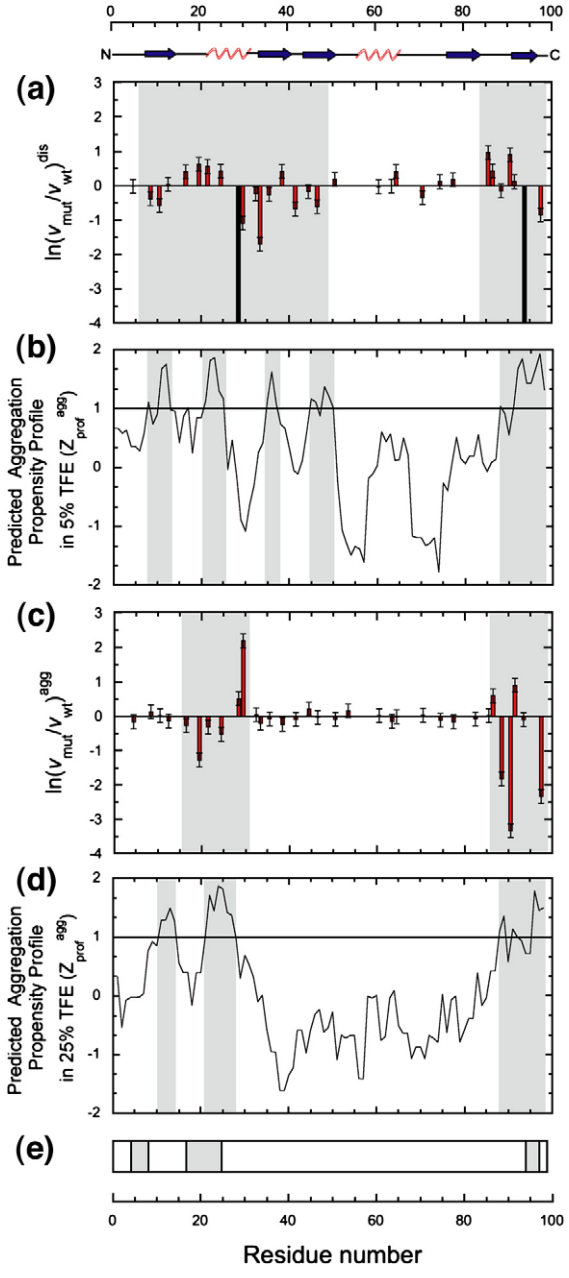

Fig. 3. (a) Changes in disaggregation rate upon mutation [$\ln(v_{mut}/v_{wt})^{dis}$]. The mutants studied here are S5T, V9A, Y11F, V13A, V17A, V20A, F22L, Y25A, A30G, I33V, G34A, V36A, V39A, T42A, G45A, V47A, V51A, M61A, W64F, L65V, P71A, I75V, T78S, I86V, S87T, L89A, Y91Q, S92T and Y98Q. v^{dis}_{mut} and v^{dis}_{wt} are the mean values of the results obtained from ThT and intrinsic fluorescence experiments. F94L and E29D did not disassemble within the time used for the experiments and are reported as black bars. Shaded areas indicate regions in which mutations have a significant impact on the disaggregation rates. Error bars, SD. (b) Aggregation propensity profile of unstructured wild-type AcP in 5% TFE, predicted using the modified version of the Zyggregator algorithm.[26,31] Regions with Z_{agg} values higher than 1 (i.e., with aggregation propensities greater than expected for a random sequence of amino acids) are considered as significantly aggregation prone and shown as shaded areas. (c) Changes in aggregation rate upon mutation [$\ln(v_{mut}/v_{wt})^{agg}$]. Shaded areas indicate the region where these changes are significant. The data are those reported in and taken with permission from Ref. 17. (d) Aggregation propensity profile of unstructured wild-type AcP in 25% TFE; shaded areas indicate regions of high aggregation propensity Z_{agg} >1. (e) Shaded areas correspond to regions of partially folded AcP sensitive to proteolysis as described in Ref. 19.

mutation mostly overlap with those with a high predicted intrinsic aggregation propensity in 5% TFE.

Regions governing the aggregation into protofibrils

Fig. 3c shows the results of a previous study that examined the effect of the 31 mutations explored here on the rate of aggregation of AcP in 25% TFE.[17] That study led to the identification of two specific regions that are more sensitive to mutation than the rest of the sequence, namely, residues 16–31 and 87–98 (Fig. 3c). In the aggregation propensity profile of AcP, calculated in the presence of 25% TFE, the regions spanning residues 11–14, 22–27 and 88–98 were predicted to have a strong tendency to aggregate (Fig. 3d). Two of these three peaks correspond, to a good approximation, to the regions 16–31 and 87–98 that were found to promote aggregation from the mutational study (Fig. 3c and d). However, from experiments the region 11–14 did not appear to be so relevant (Fig. 3c and d,).

The region spanning residues 7–14, similarly to the region encompassing residues 42–53, has been shown to be highly structured in the transition state of AcP.[32] Despite having a high intrinsic propensity to aggregate, residues 11–14 are not involved in the rate-determining steps of the aggregation process, probably because they are located in structured regions of the partially unfolded state before aggregation.[17] This hypothesis is supported by limited proteolysis experiments on the partially unfolded state of AcP populated under aggregation conditions in 25% TFE, which show that residues 9–14 are substantially more resistant to proteases, and therefore less solvent-exposed and less flexible, than residues 16–31 and 87–98 (Fig. 3e).[19]

In conclusion, the analysis shows that the regions of the sequence that promote aggregation in 25% TFE need to fulfil two requirements: to have a sufficiently high propensity to aggregate and to be sufficiently solvent-exposed and flexible to allow intermolecular interactions to occur. Such regions are limited to residues 16–31 and 87–98 in AcP.

Structural reorganisation of the AcP protofibrils preceding or following a change in solution conditions

The regions of AcP that promote aggregation in 25% TFE correspond in large part to those residues (16–31 and 87–98) that, in addition to having a high predicted aggregation propensity, are significantly exposed to solvent and flexible in the partially unfolded ensemble present prior to aggregation. Here, we have shown that the regions that play a key role in the disaggregation of AcP protofibrils in 5% TFE are more extended than those promoting aggregation in 25% TFE and include additional residues, such as those at positions 8–14, 35–38 and 45–50. Note that these regions have a high predicted intrinsic aggregation propensity in 5% TFE. These findings are summarised schematically in Fig. 4.

Two scenarios can account for the observations emerging from the comparative analysis between aggregation and disaggregation. In the first scenario, the formation of AcP protofibrils in 25% TFE might consist of two steps in which formation of the first intermolecular contacts is followed by a second phase in which other portions of the sequence are recruited into the developing β-structure. Other aggregation propensity algorithms, such as TANGO[27] and PASTA,[29] predict the region corresponding to residues 30–43 as the most likely, in the absence of TFE, to stabilize the cross-β core of amyloid aggregates (Fig. S2). The high aggregation propensity of the region 34–53, corresponding to a β-hairpin in the native state, was previously confirmed by the high insolubility of the corresponding peptide.[17] Residues 32–49 of full-length AcP are nevertheless resistant to proteolysis in 25% TFE and do not contribute to the aggregation kinetics (Fig. 3d and e).

In this scenario, regions of high aggregation propensity that are at least partially buried within the core of the partially folded monomeric species present prior to aggregation will not be involved in the initiation of this process (rate-determining steps). These regions, by contrast, may be included subsequently in the core of the fully formed amyloid protofibrils and therefore play an important role in the stability of the resulting protofibrils and in the process of their disaggregation. This conclusion is also in agreement with the observation from far-UV circular dichroism and Fourier transform infrared spectroscopy that the protofibrillar aggregates of AcP in 25% TFE have extensive β-sheet content,[15] involving a fraction of the sequence significantly larger than that resulting only from regions initiating aggregation (16–31 and 87–98).

In the second hypothesis, our predictive algorithm suggests that a more extended portion of the AcP polypeptide chain is involved in the protofibrillar aggregates in 5% TFE relative to that participating initially in the aggregation process in 25% TFE. The conformational rearrangement of the protofibrils would occur after the samples are placed in 5% TFE and prior to, or concomitant with, the disaggregation process. Since protofibrillar aggregates are likely to be rather dynamic species, it may be possible that the structure of these species is rapidly remodelled following the change in solution conditions.

According to this scenario, only regions 16–31 and 87–98 participate in the aggregation process in 25% TFE as a result of their sufficiently high aggregation propensity and flexibility under these conditions. Following the transfer of the protofibrils from 25% TFE to 5% TFE, the aggregation propensity profile of AcP changes, with new regions of the sequence becoming aggregation-prone (compare Fig. 3b and d). As a consequence, the protofibrils undergo a structural reorganisation that allows additional regions of the sequence to become structured in the aggregates. Interestingly, disassembly of the protofibrils monitored by ThT or intrinsic fluorescence and refolding of native AcP have comparable kinetics.[22] If any structural change in the protofibrils occurs in

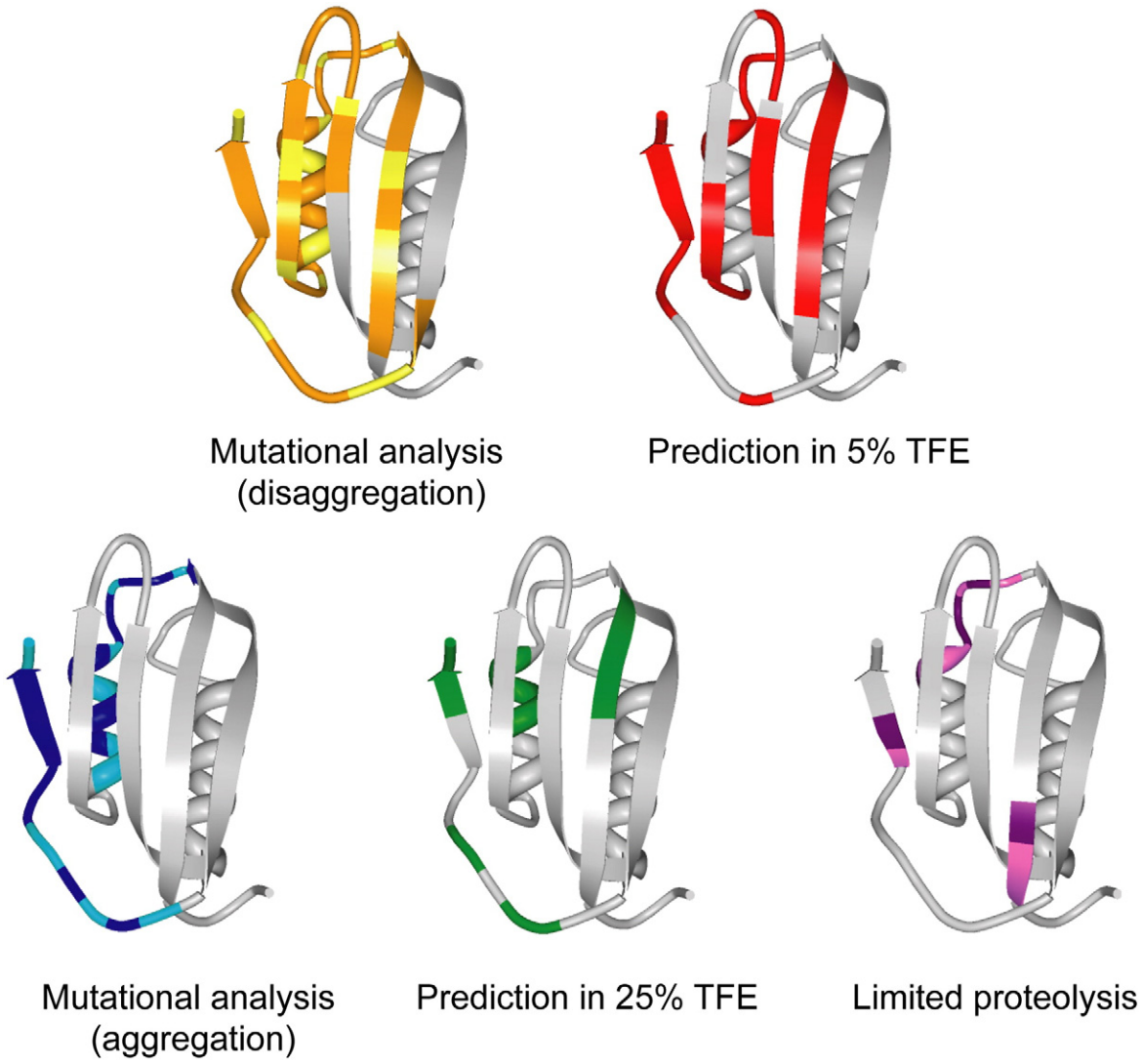

Fig. 4. Regions of the sequence that appear to promote aggregation of the partially folded ensemble (blue) or disaggregation of amyloid protofibrils (orange), as mutations within such regions significantly alter the aggregation[17] and disaggregation rates of AcP, respectively. Regions predicted to have a high aggregation propensity assuming that the unstructured protein is in 25% (green) or 5% (red) TFE.[26,31] Regions that are flexible and/or solvent-exposed in the partially folded ensemble, as probed by limited proteolysis (purple).[19] The lighter colors in some figures indicate the specific sites of mutation or proteolysis. The structure of native AcP is shown in all representations to simplify the comparisons.

the presence of 5% TFE, this is very fast and takes place within the dead time of these measurements.

Finally, an intermediate scenario between the two presented here cannot be excluded. Our results of disaggregation may result from two sequential events in which stabilisation of the protofibrils occurring in 25% TFE is followed by their structural reorganisation in 5% TFE.

Factors governing the stability of the protofibrils

There is a complex relationship between changes in disaggregation rate caused by the various mutations and changes in physicochemical parameters such as hydrophobicity and secondary structure propensity, which are linked much more directly to the aggregation kinetics. Although recent experimental studies with the $A\beta_{1-40}$ peptide[33] and computer simulations for heptapeptides[34] have indicated the significance of these factors in disaggregation, their effect is likely to be complicated by the conformational rearrangements, including the specific packing of side chains, that follow the initial aggregation step for a protein as large as AcP. Similarly to the situation that has been observed for protein folding and unfolding, aggregation and disaggregation of proteins can be governed by different factors.

In order to probe this issue further, the disaggregation rates of the 19 mutants causing changes in the net charge of AcP were analysed in detail. The mutants examined (S8H, S21R, R23Q, E29K, E29Q, E29R, S43E, S43E/K44S, S43E/K44S/R77E, K44E, K44E/R77E, Q52E, Q52E/K57Q, K88N, K88Q, E90H, S92H, R97E, R97Q) are the same as those used in previous studies on the effect of charge on the aggregation rate,[18,35] and all the amino acid substitutions were

chosen to minimise changes in hydrophobicity and secondary-structure propensity.[18,35] A strong correlation has been found between the rate constants for disaggregation and the net charge of the mutant proteins in the experiments monitored both by ThT ($R=0.73$, $p<0.001$, slope=0.64) and by intrinsic fluorescence ($R=0.61$, $p<0.01$, slope=0.29). The correlation increases even more in statistical significance when the mean of the rate constants from the two methods is considered ($R=0.82$, $p<0.0001$, slope=0.61) (Fig. 5a).

This high level of correlation can be rationalised in terms of electrostatic repulsion between molecules that promotes a higher rate of disaggregation. If mutations increase the net charge, disaggregation is faster, whereas if mutations decrease the net charge, disaggregation is slower. The contribution of solvation to this correlation appears to be negligible. The effects of mutations such as E29K or R97E on the disaggregation rate should not be attributed to changes in free energy of solvation, because the solvation would be essentially unchanged when a charged residue is replaced by another of opposite charge. According to the solvation hypothesis, the two mutations would have small or similar effects on the disaggregation process. By contrast, we observed that E29K and R97E increase and decrease the disaggregation rate, respectively.

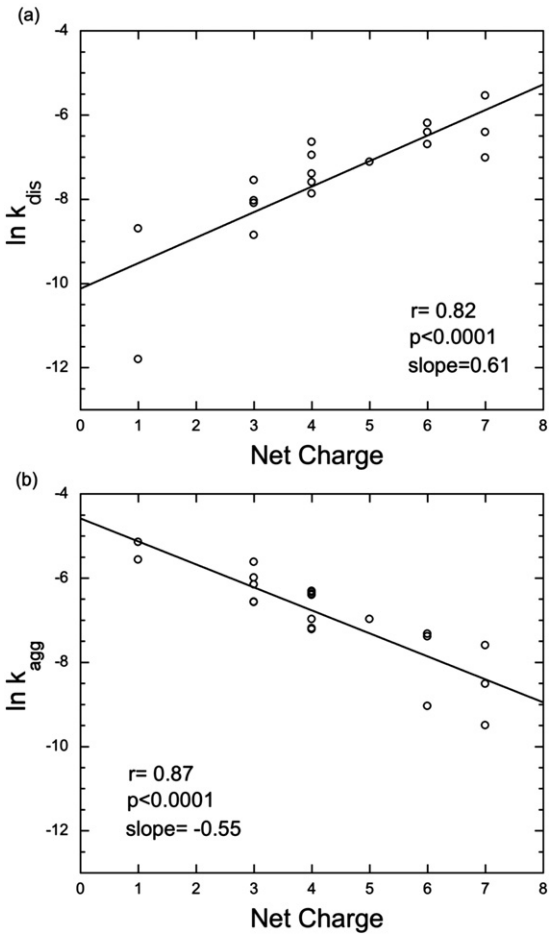

Fig. 5. Logarithm of disaggregation (a) and aggregation (b) rate constants plotted against net charge. The net charge of wt AcP is +5 under the pH studied here, while that of the mutants (S8H, S21R, R23Q, E29K, E29Q, E29R, S43E, S43E/K44S, S43E/K44S/R77E, K44E, K44E/R77E, Q52E, Q52E/K57Q, K88N, K88Q, E90H, S92H, R97E, R97Q) ranges from +1 to +7. Each k_{dis} value in (a) is the mean of the results obtained from ThT and intrinsic fluorescence experiments. Data in (b) are from ThT fluorescence experiments only and are reported in previous publications.[18,35]

As observed for the aggregation process,[18,35] the effect of changes in the protein net charge on the disaggregation rate appears to be independent of the region in which the amino acid substitution is located, at least for the specific mutations of AcP tested here, which do not involve gatekeeper residues.[31] In addition, plots of the effects of changes in net charge on disaggregation (Fig. 5a) and aggregation (Fig. 5b) rates, both obtained by ThT assays, show opposite slopes with very similar absolute values (0.64 and −0.55), indicating that changes in the electrostatic interactions have similar effects on aggregation and disaggregation. Therefore, the inverse proportionality between net charge and rate constant found for aggregation is effectively converted into a relationship of direct proportionality for disaggregation, as predicted by Tartaglia *et al.*[34] The conclusion that the overall stability of an aggregate is influenced by electrostatic interactions is also supported by previous findings that showed that neutralization of the net charge by binding of oppositely charged species (polyelectrolytes such as heparin) can increase the stability of the aggregates.[36,37]

Conclusions

We have shown that the analysis of the effects of mutations on the aggregation and disaggregation rates provides evidence for identifying the regions that contribute to the thermodynamic stability of AcP protofibrils in addition to those promoting aggregation. The methodology presented here, based on the study of the effects of conservative mutations on the rates of disruption of protein aggregates, is in principle applicable to other proteins independently of their size and initial structure. It could also be used to study different types of aggregates, such as amyloid fibrils or protofibrils. Application of this approach to investigate other systems will lead to an increasingly accurate understanding of the factors involved in the mechanism of formation of amyloid aggregates and of the way in which the forces that promote aggregation of a protein into amyloid aggregates may compete with those that induce their disassembly.

Formation and disruption of protein oligomers represent important features that determine their stability. Consequently, living organisms have evolved two ways of fighting against uncontrolled protein aggregation—by prevention of their formation (e.g., through the action of molecular chaperones such as Hsp70)[38] or by their direct disassembly

(e.g., by exploting the effects of other molecular chaperones such as Hsp104).[39] Elucidation of the factors that determine disaggregation may represent an additional approach to develop therapeutic strategies for the treatment of diseases related to protein misfolding.

Materials and Methods

Protein production and purification

Expression and purification of wild-type AcP and its variants were carried out according to the procedures described previously.[40] A QuikChange Stratagene (La Jolla, CA) kit was used for site-specific mutagenesis, and DNA sequencing was used to ensure the presence of the desired mutations. The cysteine residue at position 21 was replaced by serine in order to avoid complexities arising from the presence of a free thiol group; as in previous studies, the resulting mutant C21S is described here as the wild-type protein.[41] Similarly, all variants have the C21S substitution. Protein concentrations were measured by UV absorption using an ε_{280} value of 1.49 ml mg^{-1} cm^{-1}. For mutants in which a tyrosine or a tryptophan residue was replaced, ε_{280} values of 1.43 and 1.00 were used, respectively.

Disaggregation kinetics

Aggregation of each AcP variant was initiated by incubation of the protein at a concentration of 0.4 mg/ml in 25% (v/v) TFE and 50 mM sodium acetate buffer, pH 5.5, at 25 °C. An incubation time of 70 min was chosen for wild-type AcP because its conversion from the partially unfolded ensemble to protofibrillar aggregates is essentially complete within this time period[17] and no significant structural or size differences in the species present in solution are observable between 60 and 90 min.[22] The time of incubation for each mutant was calculated as $t^{mut} = t^{wt} k_{agg}^{wt} / k_{agg}^{mut}$, where k_{agg} is the apparent rate constant of aggregation and t^{wt} is 70 min. The proteins were then diluted fivefold with 50 mM sodium acetate buffer, pH 5.5, to 0.08 mg/ml protein, 5% (v/v) TFE.

ThT assay

Aliquots (300 μl) of each sample were withdrawn at regular time intervals and mixed with 200 μl of 50 mM acetate buffer, pH 5.5, 25 °C, containing 110 μM ThT. A Varian Cary Eclipse spectrofluorimeter (Palo Alto, CA) with excitation and emission wavelengths of 440 and 485 nm, respectively, was used to determine ThT fluorescence values. Single-exponential functions were fitted to the kinetic plots reporting the measured ThT fluorescence *versus* time in order to determine the apparent disaggregation rate constants.

Intrinsic fluorescence

A Varian Cary Eclipse spectrofluorimeter with excitation and emission wavelengths of 280 and 344 nm, respectively, was used to record the fluorescence values of the tryptophan residues during disaggregation. Single-exponential functions were fitted to the plots of the measured intrinsic fluorescence *versus* time in order to determine the disaggregation rate constants. The time course was repeated twice for each protein variant, and the mean of the two rate constants obtained was used for subsequent analysis.

Fitting procedure

For each technique used, the fitting procedure was carried out using the general equation:

$$y(t) = \sum_{i=1}^{n} A_i \exp(-k_i t) + q$$

where $y(t)$ is the signal (ThT fluorescence or intrinsic fluorescence) recorded as a function of time; A_i and k_i are the amplitude and the rate constant of the ith phase, respectively; q is the fluorescence intensity value at equilibrium; n is the number of observed phases; k values provide a quantitative measure of the rates of aggregation (v_{agg}) or disaggregation (v_{dis}) of the mutants.

Two-tailed p values were calculated from the linear correlation coefficient parameter r and the sample size n, and the error bars in the figures represent the standard deviations such that there is a 95% level of confidence that the real values fall within them.

Predictions of aggregation propensities

An algorithm was developed here to calculate the aggregation propensities (Z_{agg}) of amino acid sequences in the presence of TFE. This algorithm is based on the Zyggregator method†, which we previously introduced to predict the intrinsic aggregation propensities of amino acid sequences by considering the physicochemical properties of amino acids.[26,31] Since the presence of TFE profoundly affects the propensities for secondary-structure formation and the hydrophobicity scale, we refitted the coefficient of the Zyggregator algorithm by using the aggregation rates of TI I27 and several of its mutational variants[42] (C. Wright, unpublished results) measured in the presence of TFE.

Acknowledgements

We are very grateful for support from the Wellcome Trust, the Royal Society, the Leverhulme Trust, the European Commission (Research Directorates, project HPRN-CT-2002-00241) and the Italian MIUR (FIRB RBNE03PX83).

Supplementary Data

Supplementary data associated with this article can be found, in the online version, at doi:10.1016/j.jmb.2008.09.003

References

1. Selkoe, D. J. (2003). Folding proteins in fatal ways. *Nature*, **426**, 900–904.

† http://www-vendruscolo.ch.cam.ac.uk/software.html

2. Cohen, F. E. & Kelly, J. W. (2003). Therapeutic approaches to protein-misfolding diseases. *Nature*, **426**, 905–909.
3. Chiti, F. & Dobson, C. M. (2006). Protein misfolding, functional amyloid, and human disease. *Annu. Rev. Biochem.* **75**, 333–366.
4. Serpell, L. C., Sunde, M. & Blake, C. C. (1997). The molecular basis of amyloidosis. *Cell. Mol. Life Sci.* **53**, 871–887.
5. Rochet, J. C. & Lansbury, P. T., Jr. (2000). Amyloid fibrillogenesis: themes and variations. *Curr. Opin. Struct. Biol.* **10**, 60–68.
6. Dobson, C. M. (2003). Protein folding and misfolding. *Nature*, **426**, 884–890.
7. Stefani, M. & Dobson, C. M. (2003). Protein aggregation and aggregate toxicity: new insights into protein folding, misfolding diseases and biological evolution. *J. Mol. Med.* **81**, 678–699.
8. Dobson, C. M. (1999). Protein misfolding, evolution and disease. *Trends Biochem. Sci.* **24**, 329–332.
9. Torok, M., Milton, S., Kayed, R., Wu, P., McIntire, T., Glabe, C. G. & Langen, R. (2002). Structural and dynamic features of Alzheimer's Abeta peptide in amyloid fibrils studied by site-directed spin labeling. *J. Biol. Chem.* **277**, 40810–40815.
10. Der-Sarkissian, A., Jao, C. C., Chen, J. & Langen, R. (2003). Structural organization of alpha-synuclein fibrils studied by site-directed spin labeling. *J. Biol. Chem.* **278**, 37530–37535.
11. Margittai, M. & Langen, R. (2004). Template-assisted filament growth by parallel stacking of tau. *Proc. Natl Acad. Sci. USA*, **101**, 10278–10283.
12. Williams, A. D., Portelius, E., Kheterpal, I., Guo, J. T., Cook, K. D., Xu, Y. & Wetzel, R. (2004). Mapping abeta amyloid fibril secondary structure using scanning proline mutagenesis. *J. Mol. Biol.* **335**, 833–842.
13. Shivaprasad, S. & Wetzel, R. (2006). Scanning cysteine mutagenesis analysis of abeta-(1–40) amyloid fibrils. *J. Biol. Chem.* **281**, 993–1000.
14. Ferguson, N., Becker, J., Tidow, H., Tremmel, S., Sharpe, T. D., Krause, G. *et al.* (2006). General structural motifs of amyloid protofilaments. *Proc. Natl Acad. Sci. USA*, **103**, 16248–16253.
15. Chiti, F., Webster, P., Taddei, N., Clark, A., Stefani, M., Ramponi, G. & Dobson, C. M. (1999). Designing conditions for in vitro formation of amyloid protofilaments and fibrils. *Proc. Natl Acad. Sci. USA*, **96**, 3590–3594.
16. Chiti, F., Taddei, N., Bucciantini, M., White, P., Ramponi, G. & Dobson, C. M. (2000). Mutational analysis of the propensity for amyloid formation by a globular protein. *EMBO J.* **19**, 1441–1449.
17. Chiti, F., Taddei, N., Baroni, F., Capanni, C., Stefani, M., Ramponi, G. & Dobson, C. M. (2002). Kinetic partitioning of protein folding and aggregation. *Nat. Struct. Biol.* **9**, 137–143.
18. Chiti, F., Calamai, M., Taddei, N., Stefani, M., Ramponi, G. & Dobson, C. M. (2002). Studies of the aggregation of mutant proteins in vitro provide insights into the genetics of amyloid diseases. *Proc. Natl Acad. Sci. USA*, **99**(Suppl 4), 16419–16426.
19. Monti, M., Garolla di Bard, B. L., Calloni, G., Chiti, F., Amoresano, A., Ramponi, G. & Pucci, P. (2004). The regions of the sequence most exposed to the solvent within the amyloidogenic state of a protein initiate the aggregation process. *J. Mol. Biol.* **336**, 253–262.
20. Calamai, M., Chiti, F. & Dobson, C. M. (2005). Amyloid fibril formation can proceed from different conformations of a partially unfolded protein. *Biophys. J.* **89**, 4201–4210.
21. Bemporad, F., Taddei, N., Stefani, M. & Chiti, F. (2006). Assessing the role of aromatic residues in the amyloid aggregation of human muscle acylphosphatase. *Protein Sci.* **15**, 862–870.
22. Calamai, M., Canale, C., Relini, A., Stefani, M., Chiti, F. & Dobson, C. M. (2005). Reversal of protein aggregation provides evidence for multiple aggregated States. *J. Mol. Biol.* **346**, 603–616.
23. Chiti, F., Taddei, N., Webster, P., Hamada, D., Fiaschi, T., Ramponi, G. & Dobson, C. M. (1999). Acceleration of the folding of acylphosphatase by stabilization of local secondary structure. *Nat. Struct. Biol.* **6**, 380–387.
24. Chiti, F., Stefani, M., Taddei, N., Ramponi, G. & Dobson, C. M. (2003). Rationalization of the effects of mutations on peptide and protein aggregation rates. *Nature*, **424**, 805–808.
25. West, M. W., Wang, W., Patterson, J., Mancias, J. D., Beasley, J. R. & Hecht, M. H. (1999). De novo amyloid proteins from designed combinatorial libraries. *Proc. Natl Acad. Sci. USA*, **96**, 11211–11216.
26. Pawar, A. P., Dubay, K. F., Zurdo, J., Chiti, F., Vendruscolo, M. & Dobson, C. M. (2005). Prediction of "aggregation-prone" and "aggregation-susceptible" regions in proteins associated with neurodegenerative diseases. *J. Mol. Biol.* **350**, 379–392.
27. Fernandez-Escamilla, A. M., Rousseau, F., Schymkowitz, J. & Serrano, L. (2004). Prediction of sequence-dependent and mutational effects on the aggregation of peptides and proteins. *Nat. Biotechnol.* **22**, 1302–1306.
28. Tartaglia, G. G., Cavalli, A., Pellarin, R. & Caflisch, A. (2005). Prediction of aggregation rate and aggregation-prone segments in polypeptide sequences. *Protein Sci.* **14**, 2723–2734.
29. Trovato, A., Seno, F. & Tosatto, S. C. (2007). The PASTA server for protein aggregation prediction. *Protein Eng. Des. Sel.* **20**, 521–523.
30. Conchillo-Sole, O., de Groot, N. S., Aviles, F. X., Vendrell, J., Daura, X. & Ventura, S. (2007). AGGRESCAN: a server for the prediction and evaluation of "hot spots" of aggregation in polypeptides. *BMC Bioinformatics*, **8**, 65.
31. Tartaglia, G. G., Pawar, A., Campioni, S., Chiti, F., Dobson, C. M. & Vendruscolo, M. (2008). Prediction of aggregation-prone regions in structured proteins. *J. Mol. Biol.* **380**, 425–436.
32. Chiti, F., Taddei, N., White, P. M., Bucciantini, M., Magherini, F., Stefani, M. & Dobson, C. M. (1999). Mutational analysis of acylphosphatase suggests the importance of topology and contact order in protein folding. *Nat. Struct. Biol.* **6**, 1005–1009.
33. Hortschansky, P., Christopeit, T., Schroeckh, V. & Fandrich, M. (2005). Thermodynamic analysis of the aggregation propensity of oxidized Alzheimer's beta-amyloid variants. *Protein Sci.* **14**, 2915–2918.
34. Tartaglia, G. G., Cavalli, A., Pellarin, R. & Caflisch, A. (2004). The role of aromaticity, exposed surface, and dipole moment in determining protein aggregation rates. *Protein Sci.* **13**, 1939–1941.
35. Calamai, M., Taddei, N., Stefani, M., Ramponi, G. & Chiti, F. (2003). Relative influence of hydrophobicity and net charge in the aggregation of two homologous proteins. *Biochemistry*, **42**, 15078–15083.
36. Castillo, G. M., Ngo, C., Cummings, J., Wight, T. N. & Snow, A. D. (1997). Perlecan binds to the beta-amyloid proteins (A beta) of Alzheimer's disease, accelerates A beta fibril formation, and maintains A beta fibril stability. *J. Neurochem.* **69**, 2452–2465.
37. Yamaguchi, I., Suda, H., Tsuzuike, N., Seto, K., Seki, M., Yamaguchi, Y. *et al.* (2003). Glycosaminoglycan and proteoglycan inhibit the depolymerization of

beta2-microglobulin amyloid fibrils in vitro. *Kidney Int.* **64**, 1080–1088.
38. Hartl, F. U. & Hayer-Hartl, M. (2002). Molecular chaperones in the cytosol: from nascent chain to folded protein. *Science*, **295**, 1852–1858.
39. Weibezahn, J., Schlieker, C., Tessarz, P., Mogk, A. & Bukau, B. (2005). Novel insights into the mechanism of chaperone-assisted protein disaggregation. *Biol. Chem.* **386**, 739–744.
40. Taddei, N., Stefani, M., Magherini, F., Chiti, F., Modesti, A., Raugei, G. & Ramponi, G. (1996). Looking for residues involved in the muscle acylphosphatase catalytic mechanism and structural stabilization: role of Asn41, Thr42, and Thr46. *Biochemistry*, **35**, 7077–7083.
41. van Nuland, N. A., Chiti, F., Taddei, N., Raugei, G., Ramponi, G. & Dobson, C. M. (1998). Slow folding of muscle acylphosphatase in the absence of intermediates. *J. Mol. Biol.* **283**, 883–891.
42. Wright, C. F., Teichmann, S. A., Clarke, J. & Dobson, C. M. (2005). The importance of sequence diversity in the aggregation and evolution of proteins. *Nature*, **438**, 878–881.